

# Turbulent Wing-Leading-Edge Correlation Assessment for the Shuttle Orbiter

*Rudolph A. King and Matthew P. Vaughan  
Langley Research Center, Hampton, Virginia*

## NASA STI Program ... in Profile

Since its founding, NASA has been dedicated to the advancement of aeronautics and space science. The NASA scientific and technical information (STI) program plays a key part in helping NASA maintain this important role.

The NASA STI Program operates under the auspices of the Agency Chief Information Officer. It collects, organizes, provides for archiving, and disseminates NASA's STI. The NASA STI Program provides access to the NASA Aeronautics and Space Database and its public interface, the NASA Technical Report Server, thus providing one of the largest collection of aeronautical and space science STI in the world. Results are published in both non-NASA channels and by NASA in the NASA STI Report Series, which includes the following report types:

- **TECHNICAL PUBLICATION.** Reports of completed research or a major significant phase of research that present the results of NASA programs and include extensive data or theoretical analysis. Includes compilations of significant scientific and technical data and information deemed to be of continuing reference value. NASA counterpart of peer-reviewed formal professional papers, but having less stringent limitations on manuscript length and extent of graphic presentations.
- **TECHNICAL MEMORANDUM.** Scientific and technical findings that are preliminary or of specialized interest, e.g., quick release reports, working papers, and bibliographies that contain minimal annotation. Does not contain extensive analysis.
- **CONTRACTOR REPORT.** Scientific and technical findings by NASA-sponsored contractors and grantees.

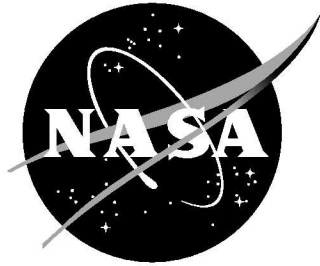
- **CONFERENCE PUBLICATION.** Collected papers from scientific and technical conferences, symposia, seminars, or other meetings sponsored or co-sponsored by NASA.
- **SPECIAL PUBLICATION.** Scientific, technical, or historical information from NASA programs, projects, and missions, often concerned with subjects having substantial public interest.
- **TECHNICAL TRANSLATION.** English-language translations of foreign scientific and technical material pertinent to NASA's mission.

Specialized services also include creating custom thesauri, building customized databases, and organizing and publishing research results.

For more information about the NASA STI Program, see the following:

- Access the NASA STI program home page at ***<http://www.sti.nasa.gov>***
- E-mail your question via the Internet to ***[help@sti.nasa.gov](mailto:help@sti.nasa.gov)***
- Fax your question to the NASA STI Help Desk at 443-757-5803
- Phone the NASA STI Help Desk at 443-757-5802
- Write to:  
NASA STI Help Desk  
NASA Center for AeroSpace Information  
7115 Standard Drive  
Hanover, MD 21076-1320

NASA/TM-2009-215949



# Turbulent Wing-Leading-Edge Correlation Assessment for the Shuttle Orbiter

*Rudolph A. King and Matthew P. Vaughan  
Langley Research Center, Hampton, Virginia*

National Aeronautics and  
Space Administration

Langley Research Center  
Hampton, Virginia 23681-2199

---

December 2009

The use of trademarks or names of manufacturers in this report is for accurate reporting and does not constitute an official endorsement, either expressed or implied, of such products or manufacturers by the National Aeronautics and Space Administration.

Available from:

NASA Center for AeroSpace Information  
7115 Standard Drive  
Hanover, MD 21076-1320  
443-757-5802

## Abstract

This study was conducted in support of the Orbiter damage assessment activity that takes place for each Shuttle mission since STS-107 (STS - Space Transportation System). As part of the damage assessment activity, the state of boundary layer (laminar or turbulent) during reentry needs to be estimated in order to define the aerothermal environment on the Orbiter. Premature turbulence on the wing leading edge (WLE) is possible if a surface irregularity promotes early transition and the resulting turbulent wedge flow contaminates the WLE flow. The objective of this analysis is to develop a criterion to determine if and when the flow along the WLE experiences turbulent heating given an incoming turbulent boundary layer that contaminates the attachment line. The data to be analyzed were all obtained as part of the MH-13 Space Shuttle Orbiter Aerothermodynamic Test conducted on a 1.8%-scale Orbiter model at Calspan/University of Buffalo Research Center in the Large Energy National Shock Tunnels facility. A rational framework was used to develop a means to assess the state of the WLE flow on the Orbiter during reentry given a contaminated attachment-line flow. Evidence of turbulent flow on the WLE has been recently documented for a few STS missions during the Orbiter's flight history, albeit late in the reentry trajectory. The criterion developed herein will be compared to these flight results.

## **Contents**

<b>1</b>	<b>Introduction</b>	<b>3</b>
<b>2</b>	<b>Overview of MH-13 WLE Data</b>	<b>3</b>
<b>3</b>	<b>Analysis Approach</b>	<b>4</b>
<b>4</b>	<b>MH-13 Correlation Results</b>	<b>5</b>
<b>5</b>	<b>Review of Flight Results</b>	<b>6</b>
<b>6</b>	<b>Conclusions</b>	<b>7</b>
	<b>References</b>	<b>8</b>
	<b>APPENDIX: NASA Internal Document</b>	<b>A-1</b>

# 1 Introduction

This document addresses the issue of turbulent heating on the wing leading edge (WLE) of the Shuttle Orbiter and was requested by the Entry Aeroheating Working Group in support of the Orbiter damage assessment activity. For the purpose of clearing the Orbiter's thermal protection system for safe reentry, the established baseline procedure used by the Data Assessment Team for assessing the state of the flow on the WLE is the same as that used for the windward surface, which incorporates the boundary layer transition (BLT) and wedge tools. Further details of the Shuttle Program approved BLT Tool V.2 and wedge tool are discussed in Refs. [1,2] and Ref. [3], respectively. This process for predicting WLE turbulence on the Orbiter may be overly conservative and is the focus of this document. Turbulence on the WLE is possible if a cavity or protruding gap filler promotes early transition and the resulting turbulent wedge flow contaminates the flow in the WLE region. To the authors' knowledge, there is no definitive evidence of turbulent flow in the WLE region of the Orbiter throughout its flight history early in the reentry trajectory. A recent review of the flight data [4] indicates that turbulent heating on the WLE may be occurring late in the trajectory (Mach numbers less than 14). The intent here is **not** to develop a correlation to predict the onset of WLE transition to turbulence. The objective of this analysis is to develop a criterion to determine if and when the flow along the WLE experiences turbulent heating given an incoming turbulent boundary layer that contaminates the attachment line. The data to be analyzed were all obtained as part of the MH-13 Space Shuttle Orbiter Aerothermodynamic Test conducted at Calspan/University of Buffalo Research Center (CUBRC) in the Large Energy National Shock Tunnel facility (LENS). Refer to the test report [5] for details of the MH-13 test program and results. Laminar and turbulent boundary layer flow states on the Orbiter model were inferred from heat flux measurements. Based on observations made during the test program, it was the first author's belief that the flow divergence along the attachment line was, at least partially, responsible for what appears to be a relaxation of the flow back to the laminar heating values along the WLE, i.e., the flow conditions at the attachment line did not enable self-sustained turbulence.

# 2 Overview of MH-13 WLE Data

The data used in this analysis were all acquired in the CUBRC LENS-I Shock Tunnel during the MH-13 test program [5,6]. The highly instrumented 1.8%-scale Orbiter model ( $L_{ref} = 23.04$  inch – distance from nose to body-flap hinge) was tested at conditions similar to reentry flight conditions (no high temperature effects). Figure 1 shows a schematic of the sensor layout on the model. The sensors of primary focus for this portion of the test program are the leading-edge heat transfer gauges on the port side of model. The gauges were installed on pyrex inserts (labeled as sections A – M) where detail layouts are given on the lower left corner of the figure. Diamond-shaped boundary layer trips were placed at upstream locations on the model and tested at flow conditions such that the flow transitioned from a laminar state to a turbulent state immediately downstream of the trips. Some configurations included a series of staggered trips on either the centerline (CL) region, the attachment-line (AL) region, or both regions on the model. A list of the set of runs and conditions used in this analysis for the test cases conducted with boundary layer trips to evaluate the WLE heating is provided in Table 1 (for a complete list see Ref. [5]). The numbers in columns CL and AL in the table represent the number of trips used in a staggered arrangement. As an example, a photograph of the model with the trip configuration for run 78 is shown in Figure 2. All conditions analyzed in this report were conducted at zero yaw and  $40^\circ$  angle of attack. Spreading of the turbulent boundary layer flow ensued downstream of the trip on the windward acreage surface and eventually contaminated the attachment-

line regions. A necessary condition here for turbulent WLE heating is the ability of the attachment-line flow to maintain turbulence as the flow diverges along the WLE. The data demonstrated that the state of the boundary layer on the WLE not only depends on the state of the incoming boundary layer flow but on the tunnel flow conditions. In some cases with the same trip configurations and an incoming turbulent boundary layer, the WLE flow was laminar and under other tunnel conditions it was turbulent. The data suggested that the state of the WLE boundary layer has at least a Reynolds number dependence.

### 3 Analysis Approach

The analysis looks at several parameters with the main emphasis being on the attachment-line Reynolds number as developed by Poll [7]. For incompressible flow, Poll defined the attachment-line Reynolds number  $\bar{R}$  as

$$\bar{R} = u_e \eta / \nu_e. \quad (1)$$

Here,  $u_e$  is the spanwise boundary layer edge velocity along the attachment line and  $\nu_e$  the kinematic viscosity at the boundary layer edge. The local length scale  $\eta$  is defined as

$$\eta = \left[ \frac{\nu_e}{(dv_e/dy)_{y=0}} \right]^{1/2} \quad (2)$$

where  $(dv_e/dy)_{y=0}$  is the velocity gradient normal to the attachment line evaluated at the edge of the attachment-line boundary layer,  $y = 0$ . A sketch depicting the attachment-line flow, coordinate system, and relevant parameters along the leading edge of a long swept wing is given in Figure 3. This sketch represents a classical attachment-line flow for an essentially zero angle-of-attack configuration where the attachment line coincides with the WLE. All parameters in Eqs. 1 and 2 are local to Figure 3. Poll demonstrated that at relatively low values of  $\bar{R}$  with incoming turbulence, the turbulent bursts decay rapidly as the flow is convected in the spanwise direction. It becomes necessary to increase the freestream Reynolds number to move the front (upstream of which turbulent bursts exist) to greater spanwise distances. The need to increase the freestream Reynolds number ends dramatically when  $\bar{R}$  approaches 245, as this is the critical Reynolds number beyond which the turbulence is self-sustaining. Poll [8] later proposed that this incompressible criterion be applied to compressible flow with the use of a reference temperature given by  $T_* = T_e + 0.1(T_w - T_e) + 0.6(T_r - T_e)$  where  $T_e$ ,  $T_w$ , and  $T_r$  are the boundary layer edge temperature, wall temperature, and recovery temperature, respectively. The compressible form of the attachment-line Reynolds number is denoted as  $\bar{R}_*$ . Poll [9] suggested a critical Reynolds number of  $\bar{R}_* = 245 \pm 35$  beyond which the burst of turbulence is self-sustaining. Poll's criterion was later validated by Benard *et al.* [10] for attachment-line transition induced by gross disturbances at  $M_e = 3.28$  in a low enthalpy hypersonic wind tunnel. Poll demonstrated this criterion for edge Mach numbers up to  $M_e = 6$ , which is well beyond the  $M_e$  values for the LENS data used in this study ( $M_e < 2.5$ ) and  $M_e$  values experienced by the Orbiter during reentry.

Estimates of the attachment-line Reynolds numbers,  $\bar{R}$  and  $\bar{R}_*$  were computed using the existing LENS database for the test conditions given in Table 1. Tecplot<sup>®</sup> and a NASA-developed program that interpolated boundary layer edge conditions were the tools used to estimate these Reynolds numbers. Details of the calculation approach are given in a NASA internal document<sup>1</sup> which is included in the appendix of this document for completeness. The Reynolds numbers were computed corresponding to the sensor locations

<sup>1</sup>Vaughan, M. P., Mazaheri, A., and Wood, W. A., "Calculating Similarity Parameters to Predict Boundary Layer Transition on the Space Shuttle Orbiter," August 7, 2008.



given in Table 2. The locations  $X$ ,  $Y$ , and  $Z$  are in the Orbiter coordinate system and are consistent with coordinates given in Figure 1 ( $X$  - streamwise distance with origin upstream of Orbiter nose,  $Y$  - spanwise distance from plane of symmetry, and  $Z$  - wall-normal distance). Note that for simplicity the Reynolds numbers were not computed for every insert (i.e., sections A, B, C – M) but were computed at every other sensor to include the full spatial extent of the insert locations.  $\bar{R}$  and  $\bar{R}_*$  were computed on the attachment line so it was necessary to project a streamline from the attachment line to each sensor location provided in the table. A plot depicting the computed attachment lines for the three nominal Mach numbers tested relative to the desired sensor locations (see Table 2) is shown in Figure 4. A detail view of section A is also included in the figure to give additional perspective. The coordinates  $x$  and  $y$  are measured from the nose and centerline, respectively. Note that the attachment-line locations in the region of interest are insensitive to freestream Mach number for the range of Mach numbers tested. Also, note the location of the attachment line relative to the WLE at  $40^\circ$  angle of attack in comparison to Figure 3. For section A, the sensor depicted in the figure just outboard of the attachment line is sensor 102 (attachment line located between sensors 102 and 103).

## 4 MH-13 Correlation Results

Plots of normalized heat flux,  $St \cdot Re_{L_{ref}}^n$ , versus the  $z_{wle}$  were plotted for all three nominal Mach numbers,  $M = 10, 14$  and  $16$ , at each insert section. For the normalized heat flux,  $St$  is the Stanton number and  $Re_{L_{ref}}$  is the freestream length Reynolds number. Following the scaling analogy for boundary layers on flat plates, the exponents  $n = 1/2$  and  $n = 1/5$  are for laminar and turbulent scaling, respectively (see for example Ref. [11]). The abscissa is defined as  $z_{wle} = (Z - Z_{wle})/L_{ref}$ ; consequently,  $z_{wle} < 0$  represents locations on the lower surface,  $z_{wle} > 0$  on the upper surface and  $z_{wle} = 0$  on the WLE of the Orbiter. As a demonstration example, Mach 10 data for a range of Reynolds numbers, with and without trips, are presented for insert section E in Figures 5 and 6 corresponding to laminar and turbulent scaling. As expected, in both figures the heating is higher on the lower surface with peak heating occurring just two to three sensor locations below the WLE ( $z_{wle} = 0$ ). In Figure 5 with the laminar scaling, there is data collapse of the normalized heat flux between runs 71 and 74 (laminar baseline runs with smooth OML - outer mold line) and run 30 (run with effective boundary layer trips), except for the few inboard sensors on the windward surface. This suggests laminar WLE heating for run 30 even with an incoming turbulent boundary layer on the windward acreage. Note that the normalized heat fluxes for all runs tend to collapse with the laminar baselines on the upper leeward surface (this is consistent for all Mach numbers tested) indicating laminar flow on the leeward side. Similarly for Figure 6 with the turbulent scaling, the data of the normalized heat flux for runs 35, 79, and 81 (runs with effective boundary layer trips) and run 132 (high Reynolds number turbulent baseline run with smooth OML) tend to collapse indicating a turbulent WLE. This process of plotting the laminar and turbulent normalized heat flux for each insert section (A – M) and for all Mach numbers tested was conducted to evaluate the state of the boundary layer near the WLE region. It is important to note that the interpretation of the state of the attachment-line boundary layer is based on the laminar versus non-laminar/turbulent normalized heat transfer data near the attachment-line region and not over the entire insert. A more complete set of plots can be found in Section 4.2 of Ref. [5] (i.e., Figures 121 - 145).

All the data to be presented from this point forward are for test cases with effective boundary layer trips as listed in Table 1. Values of the attachment-line Reynolds number  $\bar{R}$  are plotted versus  $x/L_{ref}$  values along the attachment line in Figure 7 for the three Mach numbers tested. The open symbols in all subsequent plots represent predominantly laminar heating in the WLE region. Similarly, the filled symbols represent predominantly turbulent

(or non-laminar) heating in the WLE region. There is some variation in the  $\bar{R}$  values with streamwise location as seen in Figure 7. A simple arithmetic mean of the attachment-line Reynolds number,  $\langle \bar{R} \rangle$ , for the eight locations in Table 2 is computed for each run and a similar plot is presented in Figure 8. The uncertainty of the threshold value is large due to the limited number of freestream unit Reynolds numbers tested during the WLE turbulent heating phase of the test program. From this sparse set of data, run 30 at  $M = 10$  provides an  $\bar{R}$  value where the flow over the WLE had predominantly laminar heating values, i.e., the WLE flow reverted to laminar flow. Conversely, run 126 at  $M = 14$  provides a value of  $\bar{R}$  where the WLE flow remained predominantly turbulent. It should be noted that the Mach 14 data, runs 78 and 126, are predominantly turbulent in the WLE region but clearly show evidence of relaxing to laminar heating levels downstream of insert section I. At Mach 10, run 35 demonstrated turbulent flow (or at least non-laminar heating) along the entire measured WLE region (sections A – M). These figures suggest that a threshold value for self-sustaining turbulence on the Orbiter exists somewhere in the range of  $261 < \bar{R} < 291$  (values from runs 78 and 35, respectively) assuming no Mach number dependence [9] for the current  $M_e$  range. Similarly, to account for compressibility, plots of the attachment-line Reynolds number  $\bar{R}_*$  evaluated at the reference temperature  $T_*$  are presented in Figures 9 and 10. These figures indicate a threshold value exists somewhere in the range of  $211 < \bar{R}_* < 232$ . Remarkably, this Orbiter threshold value is within the range reported by Poll [8] of  $\bar{R}_* = 245 \pm 35$  ( $210 < \bar{R}_* < 280$ ). Based on the limited sub-scale Orbiter data, the results suggest that Poll's  $\bar{R}_*$  formulation may be a viable approach to assess the state of the flow in the WLE region. However, conservatism needs to be built in to the threshold value of  $\bar{R}_* \approx 245$  as this represents a Reynolds number that enables self-sustained turbulence. That is, limited runs of turbulent flow along the WLE can exist for values of  $\bar{R}_* < 245$  that can expose portions of the WLE to significantly higher heating levels.

Because of the added complexity in computing the  $\bar{R}$  and  $\bar{R}_*$ , is it possible to correlate with a parameter already available in the wind-tunnel and flight tools? It can be shown that  $\bar{R}_*$  is related to the momentum thickness Reynolds number  $R_\theta$ , which is readily available. Figures 11 and 12 show plots of  $R_\theta$  and  $\langle R_\theta \rangle$ , respectively, along the attachment line. These figures suggest that a threshold value exists somewhere in the range of  $120 < R_\theta < 133$ . Similarly, plots of the version 1 BLT parameter [12],  $R_\theta/M_e$ , are presented in Figures 13 and 14. These figures suggest that a threshold value exists somewhere in the range of  $61 < R_\theta/M_e < 69$ . The relationship between the parameters  $\bar{R}_*$  and  $R_\theta$  is clearly geometry specific and depends on how the length scales  $\eta$  and  $\theta$  are connected. Clearly, more Orbiter-specific data are necessary to evaluate this  $R_\theta$  approach, particularly any historical flight data.

## 5 Review of Flight Results

As a result of the findings in this study, the Entry Aeroheating Working Group requested a review of the historical Orbiter flight data to evaluate if any evidence of non-laminar/turbulent heating on the WLE has been experienced during reentry by the Shuttle Orbiter [4]. To recap Ref. [4], a limited set of WLE heating measurements has been obtained on past STS missions. These flights were limited to OV-102 (Columbia) and OV-103 (Discovery) vehicles which were instrumented with a radiometer embedded in panel 9 (near the location of maximum WLE heating) of the RCC (reinforced carbon-carbon) panels on the port wing. The study also corroborated measurements of thermocouple data on the windward surface in the vicinity (both upstream and downstream) of the port wing and post flight reports to identify if earlier-than-nominal transition occurred on the windward acreage that eventually contaminated the WLE region. For flights that satisfied those conditions, the transition onset times from entry interface (EI) based on abrupt increases in radiometry measurements

attributed to laminar-to-turbulent transition were documented and  $\bar{R}_*$  values computed (see Ref. [13] for computation details).

Three missions were identified in the report, STS-48, STS-56, and STS-102 (all on OV-103). As a baseline configuration with nominal reentry transition, the results for STS-114 was also documented in the report. The results are succinctly summarized in Table 3. For the three flight cases documented in the table with earlier-than-nominal transition, turbulent heating on the Orbiter was observed at  $\bar{R}_*$  values ( $283 < \bar{R}_* < 401$ ) larger than for Poll's criterion ( $\bar{R}_* = 245 \pm 35$ ) and the analysis presented herein ( $211 < \bar{R}_* < 232$ ). No historical Orbiter flight cases have been identified where transition occurred very early in the reentry trajectory such that computed  $\bar{R}_*$  values are less than 245 as a means to anchor a threshold value with historical flight data.

## 6 Conclusions

The objective of this analysis was to develop a criterion to determine if and when the flow along the WLE experiences turbulent heating given that an incoming turbulent boundary layer contaminates the attachment line. The data analyzed were all obtained in the LENS facility. It is believed that the  $\bar{R}_*$  framework is a promising/workable approach to this problem as it is well documented in the literature. In this framework, one may need to assess how to compute a reference temperature  $T_*$  for non-equilibrium reacting-flow with species for actual flight conditions. A process was developed in Ref. [13] to evaluate  $\bar{R}_*$  on the Orbiter WLE using existing reacting-flow CFD simulations. Concerns and questions raised by a peer-review panel about the procedure used to compute  $\bar{R}_*$  are addressed in Ref. [14]. The recent review of turbulent WLE heating experienced in flight at earlier-than-nominal Orbiter transition indicates turbulent heating for  $\bar{R}_* > 283$ , consistent with the findings in this report. An alternative  $R_\theta$  framework was presented that does not necessitate the need to recompute any new parameters. Additional data are strongly recommended before adopting this  $R_\theta$  framework and, if possible, any future WLE turbulence data must be acquired at more refined unit freestream Reynolds number increments to reduce the threshold uncertainties. Any additional high-Mach-number flight data, where the WLE was contaminated with incoming turbulence from the windward surface, will be greatly instrumental in validating the  $\bar{R}_*$  criterion which was formulated on ground-based data.

## References

1. King, R. A., Kegerise, M. A., and Berry, S. A., "Version 2 of the Protuberance Correlations for the Shuttle-Orbiter Boundary Layer Transition Tool," NASA TP-2009-215951, December 2009.
2. Kegerise, M. A., King, R. A., and Berry, S. A., "Development of Cavity Induced Boundary-Layer Transition Correlations for Version 2.0 of the BLT Tool," Engineering Note EG-SS-07-05, NASA Johnson Space Center, March 2007.
3. McGinley, C. B., Berry, S. A., Kinder, G. R., Barnwell, M., Wang, K. C., and Kirk, S. K., "Review of Orbiter Flight Boundary Layer Transition Data," AIAA Paper 2006-2921, June 2006.
4. Berger, K. T., "Space Shuttle Wing-Leading-Edge Flight Data," Engineering Note EG-SS-09-04, NASA Johnson Space Center, July 2009.
5. Cassady, A. M., Bourland, G., King, R., Kegerise, M., Marichalar, J., Kirk, B. S., and Treviño, L., "MH-13 Entry II: Space Shuttle Orbiter Aerothermodynamic Test Report," NASA TP-2007-214758, July 2007.
6. Wadhams, T. P., Smolinski, G. J., Holden, M. S., and MacLean, M. G., "Experimental Space Shuttle Orbiter Studies to Acquire Data for Code and Flight Heating Model Validation," AIAA Paper 2007-551, January 2007.
7. Poll, D. I. A., "Transition in the infinite swept attachment line boundary layer," *Aero Quarterly*, Vol. 30, pp. 607-629, 1979.
8. Poll, D. I. A., "The development of intermittent turbulence on a swept attachment line including the effects of compressibility," *Aero Quarterly*, Vol. 34, pp. 1-23, 1983.
9. Poll, D. I. A., "Boundary Layer Transition on the Windward Face of Space Shuttle During Re-Entry," AIAA Paper 85-0899, June 1985.
10. Benard, E., Gaillard, L., and Roquefort, A. D., "Influence of roughness on attachment line boundary layer transition in hypersonic flow," *Experiments in Fluids*, Vol. 22, pp. 286-291, 1997.
11. Kays, W. M., and Crawford, M. E., "*Convective Heat and Mass Transfer*," 2nd ed., McGraw-Hill, New York, 1980.
12. Berry, S. A., Horvath, T.J., Greene, F. A., Kinder, G. R., and Wang, K. C., "Overview of Boundary Layer Transition Research in Support of Orbiter Return To Flight," AIAA Paper 2006-2918, June 2006.
13. Padilla, Jose F., and Wood, William A., "Calculation of Attachment Line Reynolds Number from Orbiter CFD Solution," NASA/TM 2009-215762, June 2009.
14. Wood, William A., "R-bar-star peer-review follow-up on calculation procedure," Engineering Note EG-SS-09-05, NASA Johnson Space Center, June 2009.

Table 1. MH-13 test conditions analyzed in this note with upstream diamond-shaped trips to induce turbulent WLE heating (CL - centerline and AL - attachment line).

Run No.	Nominal $M$	$Re/ft$ $10^{-6}$	Trips & Locations		
			$x/L_{ref}$	CL*	AL*
30	10	1.44	0.5	1	4 @ ea.
35	10	3.33	0.5	1	4 @ ea.
81	10	4.11	0.2	7	0 @ ea.
126	14	3.06	0.1	5	0 @ ea.
78	14	3.17	0.2	7	0 @ ea.
48	16	0.78	0.1	5	0 @ ea.

\* Multiple trips attached in a staggered arrangement.

Table 2. Locations on MH-13 Shuttle Orbiter model used to compute relevant flow parameters.

Section	Sensor No.	$X$ (inch)*	$Y$ (inch)*	$Z$ (inch)*	$x/L_{ref}$	$y/L_{ref}$
A	102	19.125	-4.099	5.254	0.6459	-0.1779
C	130	19.381	-4.324	5.271	0.6570	-0.1877
E	158	19.618	-4.557	5.285	0.6673	-0.1978
G	166	19.855	-4.796	5.299	0.6776	-0.2082
I	214	20.093	-5.034	5.312	0.6879	-0.2185
K	242	20.332	-5.274	5.326	0.6983	-0.2289
L	256	20.452	-5.395	5.333	0.7035	-0.2342
M	273	21.801	-6.738	5.396	0.7620	-0.2924

\*Locations for sensors adjacent to WLE sensors on windward surface.

Table 3. Summary of flight cases from Ref. [4].

Flight	Vehicle	Port Thermocouple BLT		Radiometer EI Time (sec)	$\bar{R}_*$
		EI Times (sec)	Mach Number		
STS-48	OV-103	1005	13.7	1020	283
STS-56	OV-103	1125-1225	10.2-7.5	1250	401
STS-102	OV-103	1065-1075	12.7-12.4	1080	307
STS-114*	OV-103	1230-1269	7.9-7.0	1275	431

\* Flight with nominal transition.

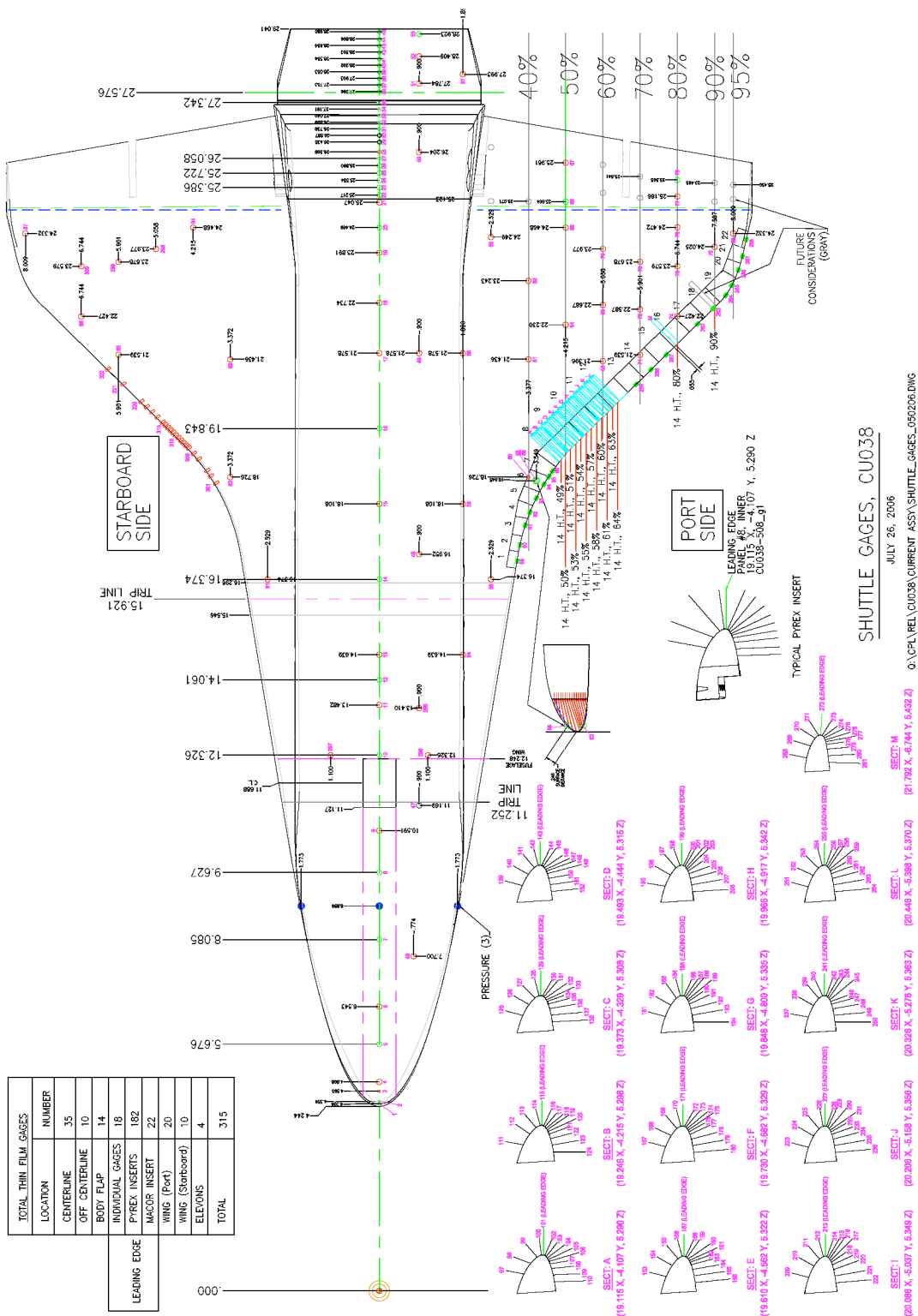


Figure 1. Sensor layout on the MH-13 1.8%-scale Orbiter model. View is from top of Orbiter model.

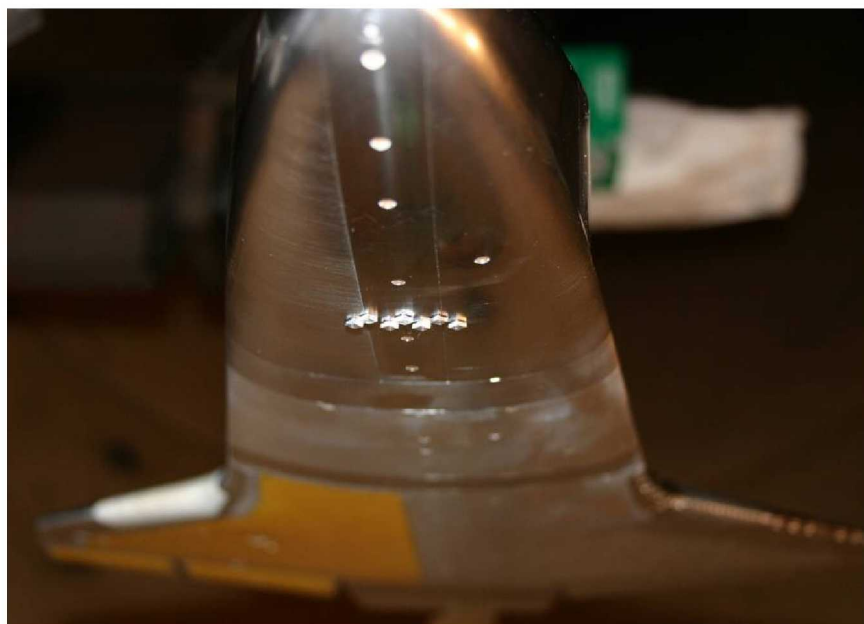


Figure 2. Trip configuration for run 78 where seven large diamond-shaped trips were in a staggered arrangement around the model centerline at  $x/L_{ref} = 0.2$ .

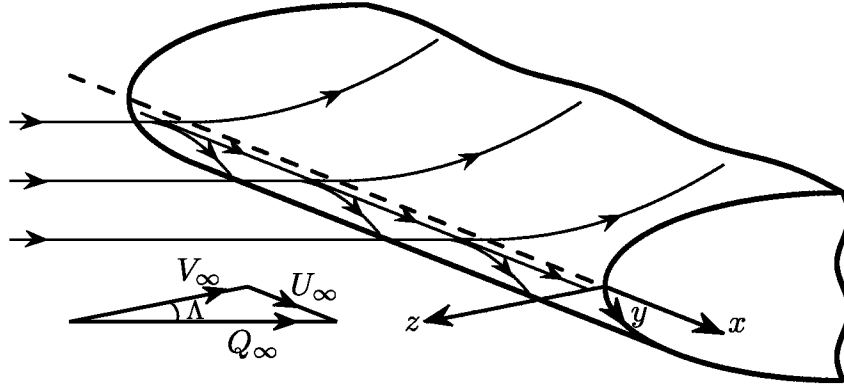


Figure 3. A classic sketch of flow near the attachment line of an infinitely swept wing at zero angle of attack.

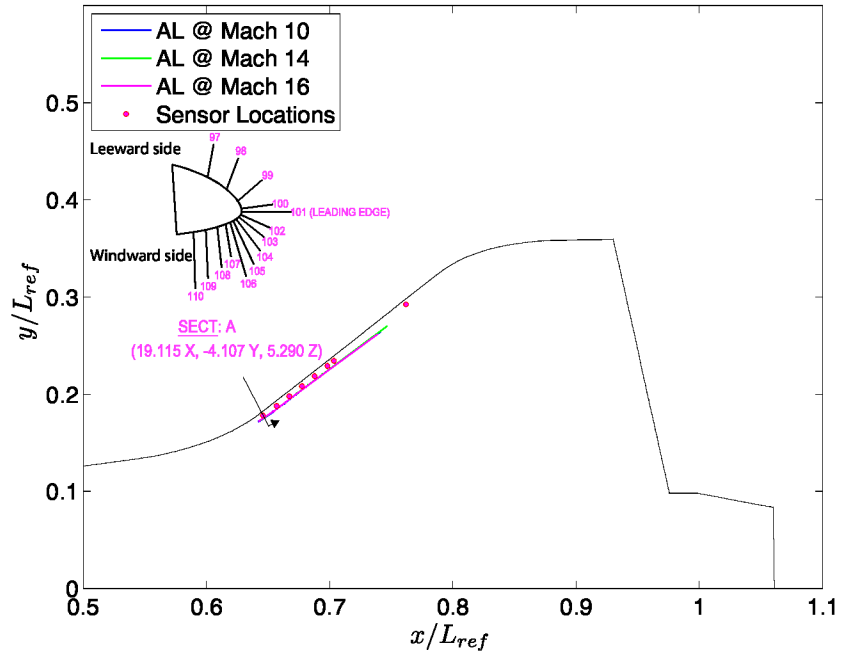


Figure 4. Sketch showing heat flux sensors (sensors adjacent to leading-edge sensors on the windward surface) relative to the attachment lines with an insert detail of section A. The attachment-line locations are insensitive to Mach number for the range shown.



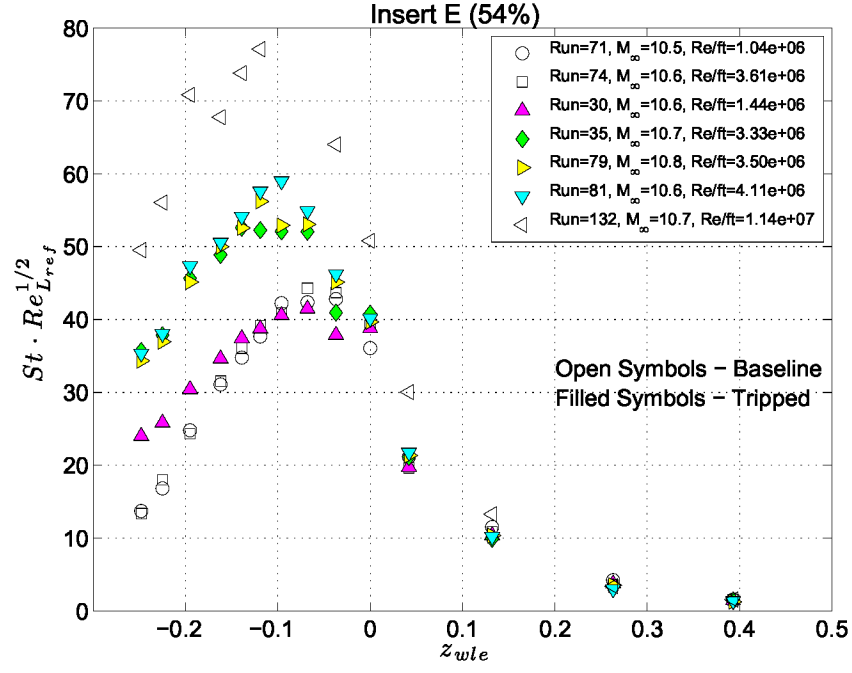


Figure 5. Example plot of normalize heat flux around the WLE at insert E to demonstrate laminar collapse at  $M = 10$ .

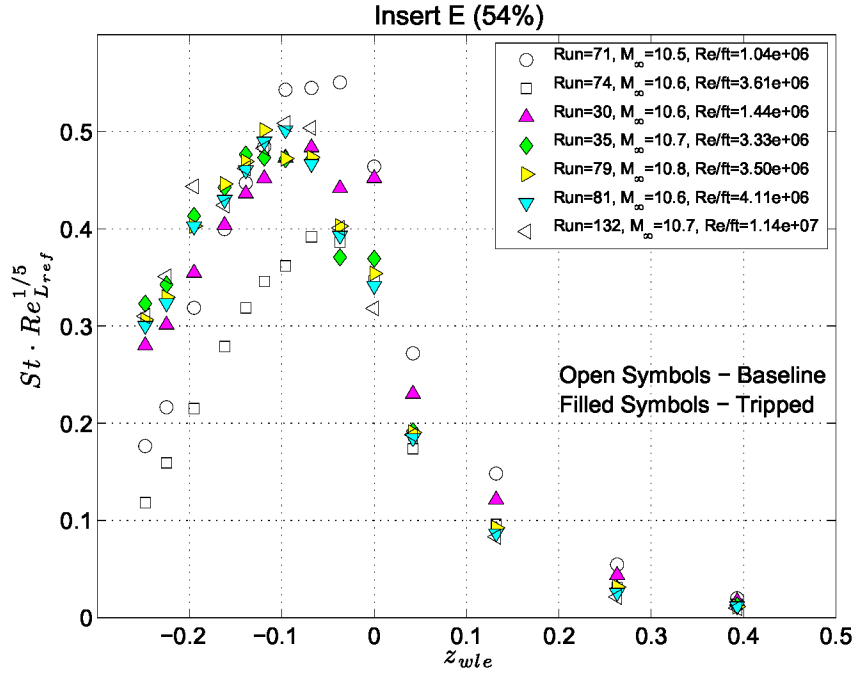


Figure 6. Example plot of normalize heat flux around the WLE at insert E to demonstrate turbulent collapse at  $M = 10$ .

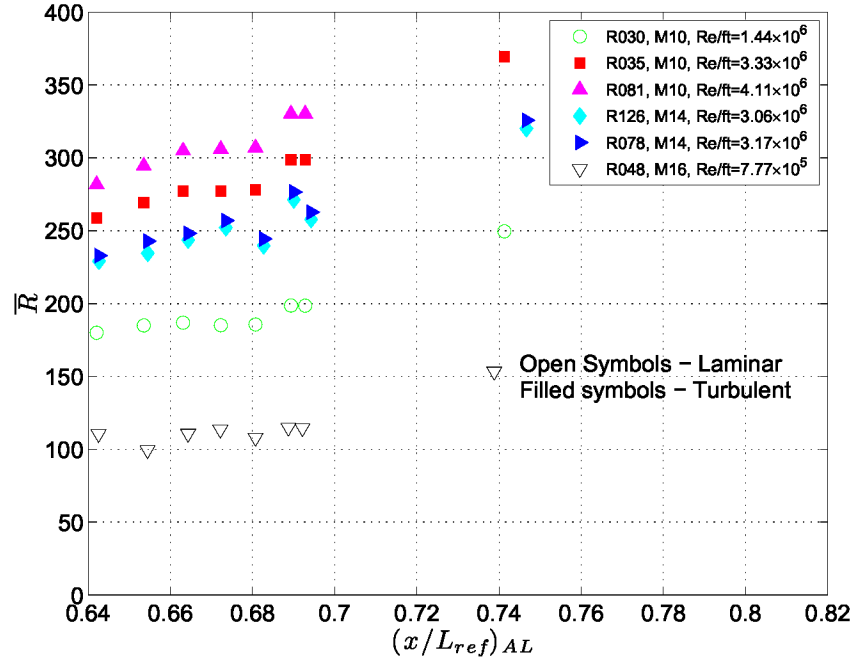


Figure 7. Attachment-line Reynolds numbers versus the attachment-line streamwise locations in the vicinity of the WLE sensors.

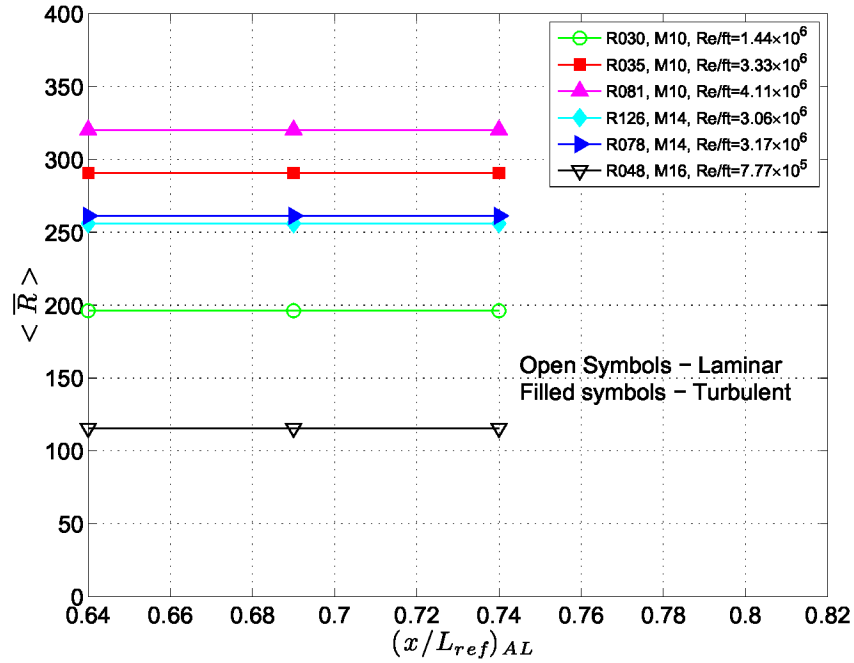


Figure 8. Average attachment-line Reynolds numbers versus the attachment-line streamwise locations in the vicinity of the WLE sensors.

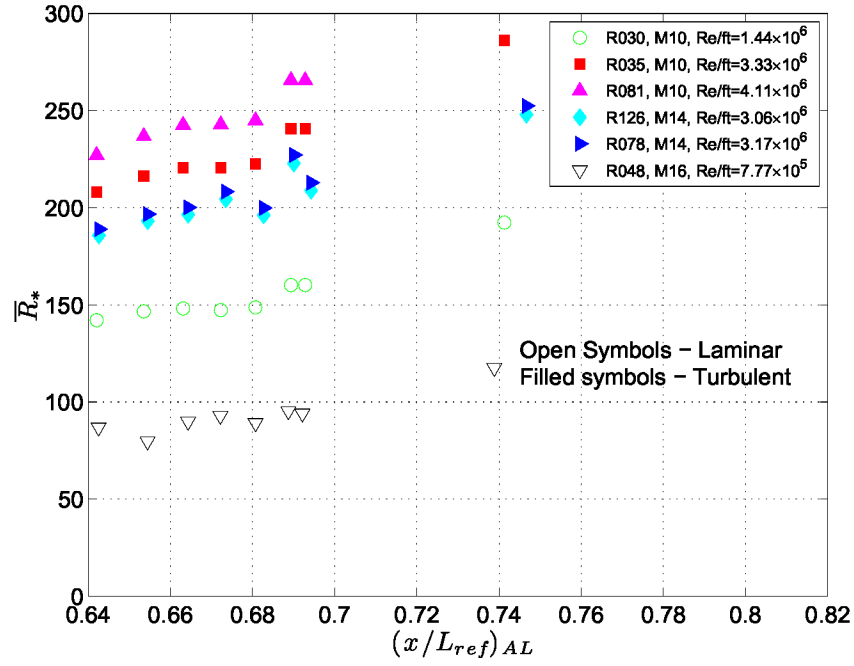


Figure 9. Attachment-line Reynolds numbers (evaluated at the reference temperature  $T_*$ ) versus the attachment-line streamwise locations in the vicinity of the WLE sensors.

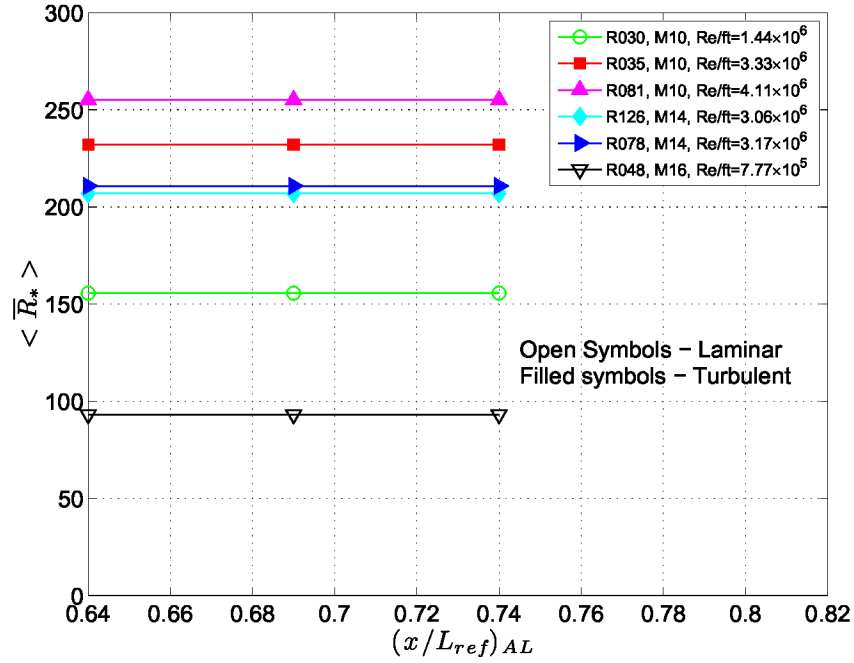


Figure 10. Average attachment-line Reynolds numbers (evaluated at the reference temperature  $T_*$ ) versus the attachment-line streamwise locations in the vicinity of the WLE sensors.

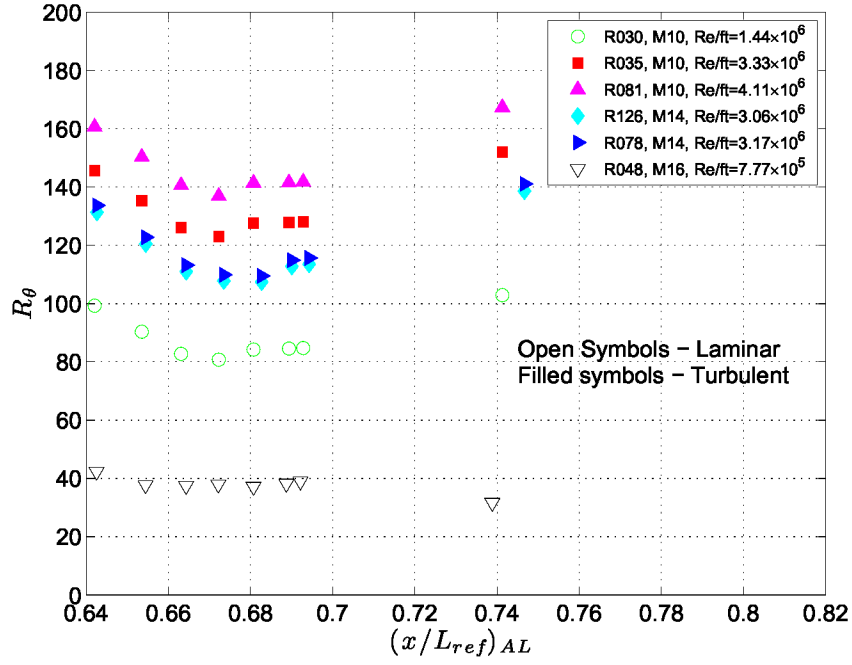


Figure 11. Momentum thickness Reynolds numbers versus the attachment-line streamwise locations in the vicinity of the WLE sensors.

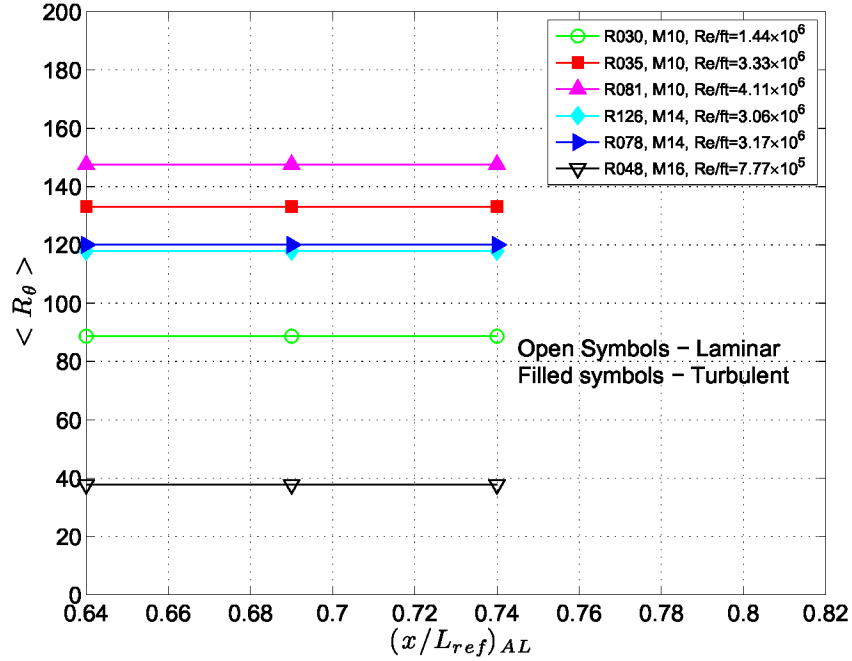


Figure 12. Average momentum thickness Reynolds numbers versus the attachment-line streamwise locations in the vicinity of the WLE sensors.

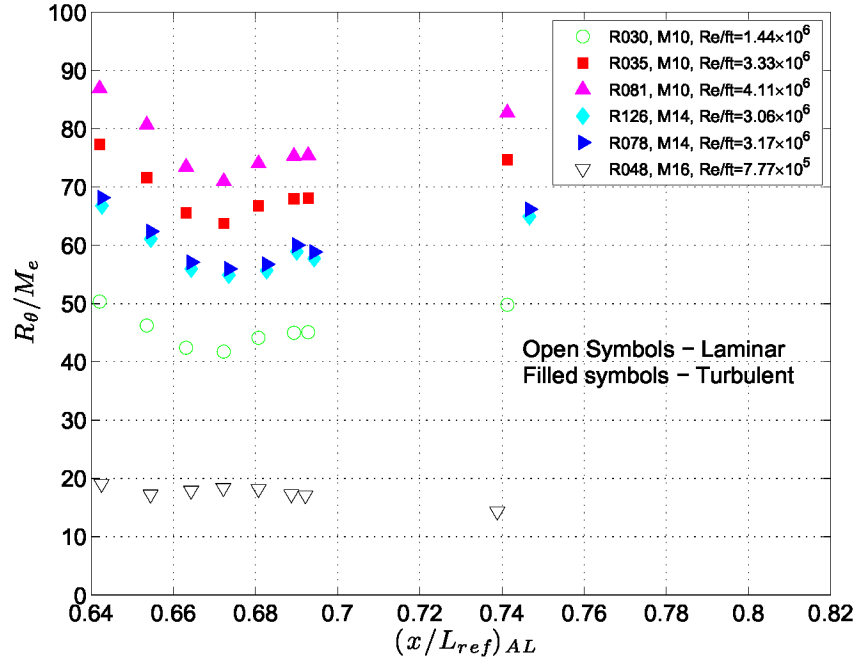


Figure 13. Momentum thickness Reynolds numbers normalized by edge Mach number versus the attachment-line streamwise locations in the vicinity of the WLE sensors.

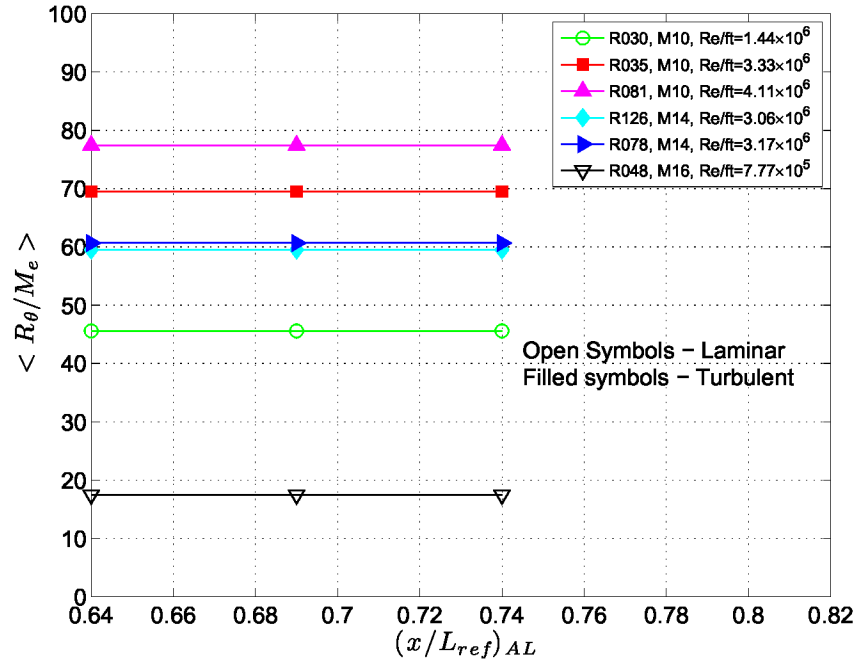


Figure 14. Average of the momentum thickness Reynolds numbers normalized by edge Mach number versus the attachment-line streamwise locations in the vicinity of the WLE sensors.

**(THIS PAGE INTENTIONALLY LEFT BLANK)**

**APPENDIX: NASA Internal Document**

**Calculating Similarity Parameters to Predict  
Boundary Layer Transition on the Space  
Shuttle Orbiter**

Matthew P. Vaughan

Alireza Mazaheri

William A. Wood

Aerothermodynamics Branch

Research and Technology Directorate

Space Operations Mission Directorate

August 7, 2008

## Abstract

The purpose of this project was to develop a method for calculating Reynolds number based similarity parameters,  $\bar{R}$  and  $\bar{R}_*$ , in an effort to more accurately predict boundary layer transition on the Wing Leading Edge (WLE) of the Space Shuttle Orbiter. These Reynolds numbers are based on boundary layer edge conditions and the velocity gradient normal to the attachment line, the line at which flow diverges toward either the leeward or windward sides of the Orbiter. The similarity parameters were calculated for several wind tunnel conditions at locations corresponding to gauges along the WLE. For the calculations, streamlines were first plotted through these locations using a program called Tecplot®. Then, attachment line points were found for each gauge location by following the streamlines until they converged to within a pre-determined threshold of  $1.25 \pm .05$  mm, corresponding to roughly three cells of the surface grid used for the analysis. Using a NASA-developed program that interpolated boundary layer edge conditions from existing wind tunnel databases, flow properties at the attachment line locations were calculated and recorded. Finally, this data yielded the desired Reynolds numbers after a few additional calculations.

After refining the method of calculation in order to reduce inconsistency and error, the two similarity parameters were easily calculated at each point for several freestream Reynolds numbers and Mach numbers. The results of the project are currently being analyzed to determine the viability of using  $\bar{R}$  and  $\bar{R}_*$  as predictors of boundary layer transition along the WLE of the Orbiter. If they correlate well to current wind tunnel data, the calculation process described in the report should be automated to rapidly characterize transition at flight conditions. An accurate prediction of boundary layer transition would allow for a less conservative but still safe approach to damage assessment, potentially saving an additional extra-vehicular activity in an already strict Space Shuttle Orbiter mission schedule to complete the construction of the International Space Station before the retirement of the fleet in 2010.

## Introduction

Upon reentry into the atmosphere, the WLE of the Space Shuttle Orbiter experiences the most severe thermal stresses on the vehicle. Thus, fast and reliable methods for characterizing the flow over the wing leading edge are critical for mission safety. One problem associated with this characterization is the transition of the boundary layer from laminar to turbulent flow, which greatly increases the rate of heat transfer to the structure. One method being investigated involves the use of two Reynolds numbers based on boundary layer edge conditions at the WLE attachment line. The attachment line marks the divergence of airflow to either the windward or leeward side of the Orbiter (see Figures A-1 and A-2). These parameters are given by the following equations (Poll, 1985):

$$\bar{R} = \left[ \frac{U_e^2}{\nu_e (dV_e/dy)_{y=0}} \right]^{1/2} \quad (\text{A-1})$$

$$\bar{R}_* = \left[ \frac{U_e^2}{\nu_* (dV_e/dy)_{y=0}} \right]^{1/2} \quad (\text{A-2})$$

In these equations,  $U_e$  is the velocity along the attachment line,  $(dV_e/dy)_{y=0}$  is the cross-wise velocity gradient at the attachment line,  $\nu_e$  is the kinematic viscosity at the boundary layer edge, and  $\nu_*$  is the kinematic viscosity evaluated at the turbulent reference temperature, given by

$$T_* = T_e + 0.10(T_w - T_e) + 0.60(T_r - T_e) \quad (\text{Poll, 1985}) \quad (\text{A-3})$$



where  $T_r$  is the recovery temperature, given by Benard, Cooper, and Sidorenko (2005) as

$$T_r = T_e \left( 1 + r \frac{\gamma - 1}{2} M_e^2 \right) \quad (\text{A-4})$$

For the calculation of  $\bar{R}$  and  $\bar{R}_*$ ,  $\gamma$  is taken to be 1.4,  $r = \sqrt{Pr}$ , and a value of 0.72 is used for  $Pr$  (White, 1974). In order to determine the dynamic viscosity at the turbulent reference temperature, Sutherlands Law was used to give

$$\frac{\mu}{\mu_0} \approx \left( \frac{T}{T_0} \right)^{3/2} \frac{T_0 + S}{T + S} \quad (\text{A-5})$$

where the subscript indicates a reference variable. For air,  $T_0 = 273.11K$ ,  $\mu_0 = 1.72 \times 10^{-5} Pa \cdot s$  and  $S = 110.56K$  (White, 1974).

The purpose of the research was to determine the feasibility of calculating  $\bar{R}$  and  $\bar{R}_*$  for several points near the WLE of the Space Shuttle Orbiter. The attachment line along the wing shifts towards the centerline of the Orbiter at high angles of incidence, deviating significantly from the attachment line of the infinite swept cylinder described by Poll (1985) and increasing the complexity of the calculation. Because the actual attachment line for the Orbiter is not precisely on the WLE, the possibility of obtaining meaningful results from any calculation method developed was unclear before the research was conducted.

All boundary layer flowfield properties used in this work were obtained from an existing database of CFD simulations. The simulations modeled the Orbiter at 40-degrees angle of attack, for various freestream Reynolds numbers corresponding to conditions tested as part of the MH-13 experiment (Cassady *et al.*, 2007). The CFD simulations were performed using the viscous flow solver Data-Parallel Line Relaxation algorithm (DPLR) (Wright *et al.*, 1998) using a 5-species air model and a constant-temperature, fully-catalytic surface.

## Data Extraction

Calculating the two similarity parameters  $\bar{R}$  and  $\bar{R}_*$  required two distinct steps. First, a plotting tool called Tecplot was used to display the windward side of a wind tunnel model of the Orbiter along with surface and boundary layer edge conditions at a particular freestream Reynolds number and Mach number. Tecplot allows precise plotting of streamlines, which is useful to locate the attachment line. Second, a NASA developed program called Blvolprops<sup>1</sup> was used to calculate surface and boundary layer edge conditions at user-specified points at a variety of Mach numbers and Reynolds numbers. The program interpolates these conditions from a database of CFD simulations of Orbiter flowfields at wind tunnel conditions, spanning the tunnel operational Reynolds-number range. Figure A-3 shows the Reynolds numbers, Mach numbers, and angles of attack used for the calculations. A Microsoft<sup>®</sup> Excel spreadsheet was also employed, facilitating data storage from the other two programs and expediting the actual calculation of  $\bar{R}$  and  $\bar{R}_*$ .

The process of calculating the two similarity parameters began with the plotting of streamlines near the tip of the Orbiters wing. The convergence of the upstream streamlines revealed the approximate location of the attachment line. Then, eight points at Mach 10, Mach 14, and Mach 16, and an additional four points at Mach 14 corresponding to gauges on a wind tunnel model were plotted along with streamlines passing through each (see Figure A-4). These streamlines rapidly converged to the position of the attachment line as they were followed upstream, and a threshold separation distance between the two of

<sup>1</sup>Meyer, B., "A Boundary Layer Probing and Reynolds Number Interpolation Tool: Blvolprops v3.0." Swales Technical Note 06-488, Hypersonic Vehicle Analysis Group, NASA Langley Research Center, November 2006.

approximately  $1.25 \pm .05$  mm was chosen, corresponding to approximately three cells on the surface grid used to analyze the model. This threshold was chosen because of the need to balance the practical application of the method and the asymptotic convergence of the streamlines upstream of gauge locations. Too small of a threshold would lead to attachment line points near the nose of the Orbiter, but a threshold that is too large would cause unacceptable discrepancies between conditions along the streamline and conditions at the attachment line. Once this threshold was crossed, the point on the attachment line was recorded in the spreadsheet and used to determine relevant parameters such as boundary layer edge temperature, pressure, viscosity, and density.

Calculating the crosswise velocity gradient at the attachment line locations found above presented the most technical difficulty as there was no automatic method for obtaining accurate values of the gradient at specific points. An initial attempt to calculate the gradient approximated the vector normal to the attachment line velocity by visual inspection. Two points were chosen along this vector, and the components of the velocity along the approximated normal at each point were recorded. The gradient was then calculated using the following relation:

$$\left( \frac{dV_e}{dy} \right)_{y=0} \approx \frac{\Delta V_{e,2} - \Delta V_{e,1}}{\Delta y} \quad (\text{A-6})$$

where  $\Delta y$  is the distance between the two points. However, the error associated with approximating the normal vector was too large and unpredictable, so a new method was developed to make the calculation more consistent.

In the new method, a vector normal to the surface was calculated through the cross product of two arbitrary vectors on the grid starting from the attachment line point. A Tecplot utility that automatically calculated the surface normal vector was later used to verify the accuracy of this method. The surface normal vector was then crossed with the velocity vector along the attachment line to produce a vector in the direction of the desired crosswise gradient. Finally, this vector was used to obtain one point on either side of the attachment line at a fixed distance of 1.25 mm. Decreasing the magnitude of the surface normal vector reduced the error resulting from the projection of the two points onto the curved surface of the wing.

Once these points were obtained, Blvolprops was used to determine the boundary layer edge velocity at each point, yielding the gradient after a few additional calculations according to equations A-1 through A-6. With this gradient and the other parameters acquired at the attachment line point,  $\bar{R}$  is easily calculated. However, the viscosity term of  $\bar{R}_*$  must be evaluated at turbulent reference conditions. Using Sutherlands Law and assuming that air is an ideal gas, the turbulent reference temperature, density, and dynamic viscosity were determined, allowing  $\bar{R}_*$  to be calculated.

## Conclusion

The calculation of  $\bar{R}$  and  $\bar{R}_*$  proceeded smoothly once the method described above was fully developed, and the research exceeded expectations due to the rapid development and implementation of the method. The requested values of the two parameters were passed on to be analyzed for potential correlations to boundary layer transition along the WLE of the Space Shuttle Orbiter. If the parameters correlate well, they could potentially be used as an additional means to assess damage on the Orbiter. Early boundary layer transition is a serious risk to the structural integrity of the Orbiter, so an accurate prediction of transition due to a damaged and irregular surface would be valuable towards determining whether repairs are needed. However, despite the relative simplicity of the calculation method, the process is tedious to perform by hand and should be automated before it is used in a real time scenario.

## References

- Anderson, (2000). Anderson, J. D., Jr. (2000). *Fundamentals of Aerodynamics (3rd ed.)*. New York: McGraw-Hill.
- Benard, *et al.*, (2005). Benard, E., Cooper, R. K., and Sidorenko, A. (2005). Transition and turbulent heat transfer of swept cylinder attachment line in hypersonic flow. *International Journal of Heat and Mass Transfer*, 49, 836–843.
- Cassady, *et al.*, (2007). Cassady, A. M., Bourland, G., King, R., Kegerise, M., Marichalar, J., Kirk, B. S., and Treviño, L. (2007). MH-13 Entry II: Space Shuttle Orbiter Aerothermodynamic Test Report. NASA TP-2007-214758.
- Poll, (1985). Poll, D. I. A. (1985). Boundary layer transition on the windward face of Space Shuttle during re-entry. AIAA Paper No. 85-0899.
- White, (1974). White, F. M. (1974). *Viscous fluid flow*. New York: McGraw-Hill.
- Wright, *et al.*, (1998). Wright, M. J., and Candler, G. V. and Bose, D. (1998). Data-Parallel Line Relaxation Method for the Navier-Stokes Equations. *AIAA Journal*, 36, 9, 1603–1609.

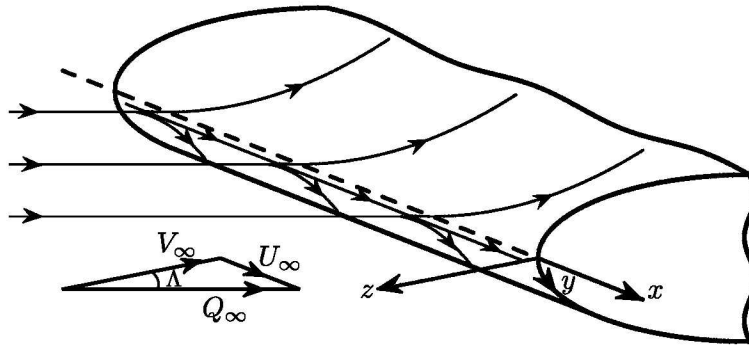


Figure A-1. Attachment line on an idealized infinite swept cylinder.

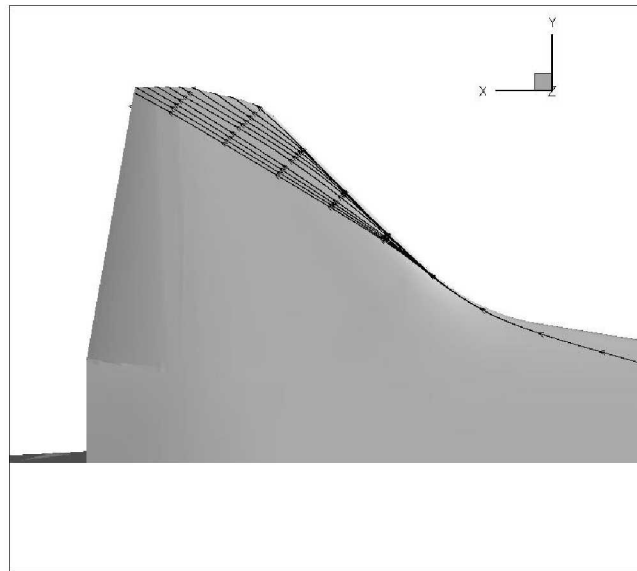


Figure A-2. Streamlines diverging from the attachment line on the Orbiter (Plotted using Tecplot).

Case	Run	Nominal Mach	Re/ft x 10 <sup>-6</sup>	AoA (deg)
1	30	10	1.44	40
2	35	10	3.33	40
3	81	10	4.11	40
4	132	10	11.4	40
5	126	14	3.06	40
6	78	14	3.17	40
7	48	16	0.78	40
8	127	16	1.12	40

Figure A-3. Table showing the wind tunnel conditions used to calculate  $\bar{R}$  and  $\bar{R}_*$ .

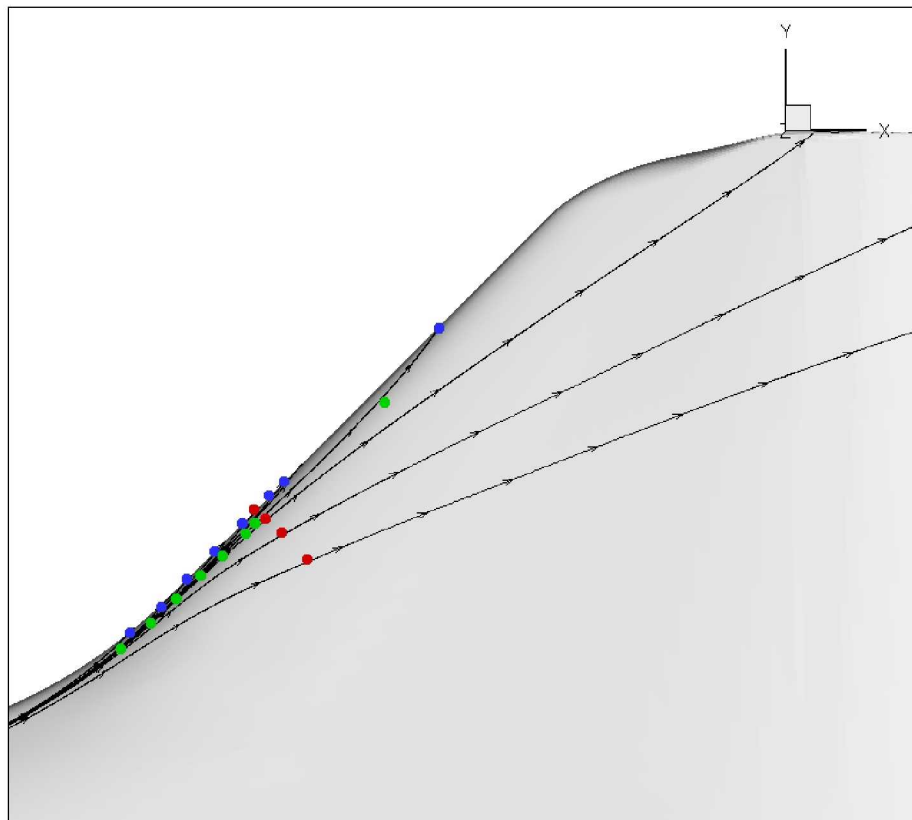


Figure A-4. Gauge locations (blue) with corresponding Mach 10 attachment line points (green). The additional four Mach 14 points are shown in red (Plotted using Tecplot).



REPORT DOCUMENTATION PAGE					Form Approved OMB No. 0704-0188	
<p>The public reporting burden for this collection of information is estimated to average 1 hour per response, including the time for reviewing instructions, searching existing data sources, gathering and maintaining the data needed, and completing and reviewing the collection of information. Send comments regarding this burden estimate or any other aspect of this collection of information, including suggestions for reducing this burden, to Department of Defense, Washington Headquarters Services, Directorate for Information Operations and Reports (0704-0188), 1215 Jefferson Davis Highway, Suite 1204, Arlington, VA 22202-4302. Respondents should be aware that notwithstanding any other provision of law, no person shall be subject to any penalty for failing to comply with a collection of information if it does not display a currently valid OMB control number.</p> <p><b>PLEASE DO NOT RETURN YOUR FORM TO THE ABOVE ADDRESS.</b></p>						
1. REPORT DATE (DD-MM-YYYY) 01-12-2009		2. REPORT TYPE Technical Memorandum		3. DATES COVERED (From - To)		
4. TITLE AND SUBTITLE Turbulent Wing-Leading-Edge Correlation Assessment for the Shuttle Orbiter				5a. CONTRACT NUMBER		
				5b. GRANT NUMBER		
				5c. PROGRAM ELEMENT NUMBER		
6. AUTHOR(S) Rudolph A. King and Matthew P. Vaughan <sup>†</sup> <sup>†</sup> Work performed under the Langley Aerospace Research Summer Scholar Program				5d. PROJECT NUMBER		
				5e. TASK NUMBER		
				5f. WORK UNIT NUMBER 599489.02.07.07.04.11.01		
7. PERFORMING ORGANIZATION NAME(S) AND ADDRESS(ES) NASA Langley Research Center Hampton, Virginia 23681-2199				8. PERFORMING ORGANIZATION REPORT NUMBER L-19784		
9. SPONSORING/MONITORING AGENCY NAME(S) AND ADDRESS(ES) National Aeronautics and Space Administration Washington, DC 20546-0001				10. SPONSOR/MONITOR'S ACRONYM(S) NASA		
				11. SPONSOR/MONITOR'S REPORT NUMBER(S) NASA/TM-2009-215949		
12. DISTRIBUTION/AVAILABILITY STATEMENT Unclassified-Unlimited Subject Category 16 Availability: NASA CASI (443) 757-5802						
13. SUPPLEMENTARY NOTES An electronic version can be found at <a href="http://ntrs.nasa.gov">http://ntrs.nasa.gov</a> .						
14. ABSTRACT This study was conducted in support of the Orbiter damage assessment activity that takes place for each Shuttle mission since STS-107 (STS - Space Transportation System). As part of the damage assessment activity, the state of boundary layer (laminar or turbulent) during reentry needs to be estimated in order to define the aerothermal environment on the Orbiter. Premature turbulence on the wing leading edge (WLE) is possible if a surface irregularity promotes early transition and the resulting turbulent wedge flow contaminates the WLE flow. The objective of this analysis is to develop a criterion to determine if and when the flow along the WLE experiences turbulent heating given an incoming turbulent boundary layer that contaminates the attachment line. The data to be analyzed were all obtained as part of the MH-13 Space Shuttle Orbiter Aerothermodynamic Test conducted on a 1.8%-scale Orbiter model at Calspan/University of Buffalo Research Center in the Large Energy National Shock Tunnels facility. A rational framework was used to develop a means to assess the state of the WLE flow on the Orbiter during reentry given a contaminated attachment-line flow. Evidence of turbulent flow on the WLE has been recently documented for a few STS missions during the Orbiter's flight history, albeit late in the reentry trajectory. The criterion developed herein will be compared to these flight results.						
15. SUBJECT TERMS Shuttle Orbiter, hypersonic boundary layer transition, attachment-line transition						
16. SECURITY CLASSIFICATION OF:			17. LIMITATION OF ABSTRACT	18. NUMBER OF PAGES	19a. NAME OF RESPONSIBLE PERSON	
a. REPORT	b. ABSTRACT	c. THIS PAGE			STI Help Desk (email: <a href="mailto:help@sti.nasa.gov">help@sti.nasa.gov</a> )	
U	U	U	UU	31	19b. TELEPHONE NUMBER (Include area code) (443) 757-5802	





